

1N-02

40307

P-17

Application of Pressure Sensitive Paint in Hypersonic Flows

Kenol Jules
*Lewis Research Center
Cleveland, Ohio*

and

Mario Carbonaro and Stephan Zemsch
*von Karman Institute for Fluid Dynamics
Rhode-St-Genese, Belgium*

February 1995



National Aeronautics and
Space Administration

(NASA-TM-106824) APPLICATION OF
PRESSURE SENSITIVE PAINT IN
HYPERSONIC FLOWS (NASA. Lewis
Research Center) 17 p

N95-20794

Unclass

63/02 0040307

7
J

Application of Pressure Sensitive Paint in Hypersonic Flows

Kenol Jules*, Mario Carbonaro** and Stephan Zemsch†

von Karman Institute for Fluid Dynamics,
72 Chaussee de Waterloo,
B-1640 Rhode-St-Genese, Belgium

SUMMARY

It is well known in the aerodynamic field that pressure distribution measurement over the surface of an aircraft model is a problem in experimental aerodynamics. For one thing, a continuous pressure map can not be obtained with the current experimental methods since they are discrete. Therefore, interpolation or CFD methods must be used for a more complete picture of the phenomenon under study.

For this study, a new technique was investigated which would provide a continuous pressure distribution over the surface under consideration. The new method is pressure sensitive paint. When pressure sensitive paint is applied to an aerodynamic surface and placed in an operating wind-tunnel under appropriate lighting, the molecules luminesce as a function of the local pressure of oxygen over the surface of interest during aerodynamic flow. The resulting image will be brightest in the areas of low pressure (low oxygen concentration), and less intense in the areas of high pressure (where oxygen is most abundant on the surface).

The objective of this investigation was to use pressure sensitive paint samples from Mc Donnell Douglas (MDD) for calibration purpose in order to assess the response of the paint under appropriate lighting and to use the samples over a flat plate/ conical fin mounted at 75° from the center of the plate in order to study the shock / boundary layer interaction at Mach 6 in the Von Karman wind-tunnel.

From the result obtained it was concluded that temperature significantly affects the response of the paint and should be

given the uppermost attention in the case of hypersonic flows. Also, it was found that past a certain temperature threshold, the paint intensity degradation became irreversible. The comparison between the pressure tap measurement and the pressure sensitive paint showed the right trend. However, there exists a shift when it comes to the actual value. Therefore, further investigation is under way to find the cause of the shift.

1. INTRODUCTION

Based on the information that have been reported in the open literature, it seems that the development and utilization of pressure sensitive paint (PSP) promise to revolutionize the art of pressure measurement in wind-tunnel testing. Currently, hundreds of thousands of pressure orifices would be required, if one wants to map an entire surface of an aircraft. Since the pressure orifices are usually separated by a significant distance, a continuous pressure map is not achieved. The technique used to determine pressures between the orifices is to interpolate them by computational fluids dynamics (CFD)^{1,2}. Therefore, a method to obtain continuous pressure data in wind-tunnels is necessary which would provide the information needed to eliminate some of the uncertainty in CFD models.

The classic tap measurements of pressure distribution are very complex and expensive due to the model itself and pressure measurement techniques. However, being able to obtain a pressure distribution in experimental aerodynamics is very important since it allows the definition of flow separation zones, shock waves positions and load distribution. It also

* Aerospace Engineer, NASA Lewis Research Center

** Head, Aeronautics/Aerospace Dept., von Karman Institute

† PhD student, von Karman Institute for Fluid Dynamics

permits the visualization of aerodynamic interference between aircraft components. In addition, it allows identification of parts of the surface which should be changed to improve the pressure distribution. Thus, generating a continuous pressure map over a surface would, indeed, revolutionize the field of aerodynamics.

In 1980, Peterson and Fitzgerald³ proposed the oxygen quenching of fluorescent dyes for flow visualization in a wind tunnel. In their experiment, the luminescent dye was absorbed onto silica particles. The coating was rough and adherence was a problem. No attempt to quantify the result was made. Since mid 80's to now, quite a few papers have been published to demonstrate the feasibility of using this method in a quantitative manner. As a result, a new method of pressure measurement was born: Pressure Sensitive Paint (PSP) measurement.

What is pressure sensitive paint? Molecular photoluminescence is the basis for this (new) technology. Photoluminescence is a mechanism by which a molecule can lose excess energy by emitting a photon and return to the ground electronic state. During this process lower energy photons are emitted, i.e, the emitted light is red shifted compared to the excitation light. Luminescence is a broad term which encompasses both fluorescence and phosphorescence. Fluorescence refers to the radiative transition of electrons from first excited singlet state to the singlet ground state ($S_1 \rightarrow S_0$). The ground state characterizes the electronic energy of the unexcited molecule. The singlet excited state is formed when the sample absorbs light. Fluorescence has a relatively short lifetime, approximately⁴ $10^{-9} - 10^{-7}$ s. Phosphorescence is a radiative relaxation of an electron from the lowest excited triplet state to the singlet ground state ($T_1 \rightarrow S_0$). The triplet excited state is formed when the electrons in the excited state change their spin. Phosphorescence has a relatively long lifetime ($10^{-4} - 10$ s). Also, due to the lower energy of the triplet state, the wavelength of phosphorescence is longer than that of the fluorescence.

Pressure sensitive paint is based on the oxygen-quenching phenomenon of luminescence of specific organic luminophores. For a given excitation level, the brightness of the luminescent material varies inversely with the partial pressure of oxygen and, hence, to the pressure of the air. When the PSP is applied to an aerodynamic surface and placed in an operating wind tunnel under appropriate lighting, the molecules luminesce as a function of the local pressure of oxygen over the surface of interest during aerodynamic flow. The resulting image will be brightest in the areas of low pressure (low oxygen concentration), and less intense in the areas of high pressure (where oxygen is most abundant on the surface). The lumines-

cence data can be used to map a continuous pressure field over/under the model under investigation. This new technique could potentially save both time and money for the aircraft industry by doing away with building a separate, complicated pressure model. All that is needed is to apply the paint on the model one wishes to study and determine which data acquisition and illumination system is best suited for the investigation.

2. THEORETICAL BACKGROUND

The Stern-Volmer relation⁵ can be used to describe the luminescence of a molecule in a solution that is subject to bimolecular quenching by another species. According to the Stern-Volmer model, the rate constant for luminescence decay in the presence of oxygen is given by:

$$K_{total} = K_r + K_n + K_q P = K_a + K_q P = \tau^{-1} \quad (1)$$

Where:

K_r = radiative lifetime of the excited state

K_n = rate of any intrinsic non-radiative decay process

K_q = the quenching rate due to collisions with oxygen

P = the oxygen pressure

K_a = the intrinsic de-excitation rate in the absence of oxygen

τ = the emission lifetime

Another important parameter which rules luminescence intensity is luminescence quantum yield:

$$\phi = (\text{photons emitted} / \text{photons absorbed})$$

$$= \frac{K_r}{K_{total}} \quad (2)$$

From equations (1) and (2) the quantum yield ϕ_0 at a reference pressure P_0 divided by the quantum yield ϕ at any other pressure P is given by:

$$\frac{\phi_0}{\phi} = \frac{K_a + K_q P}{K_a + K_q P_0} \quad (3)$$

Since the observed phosphorescence intensity I (detected intensity) under fixed conditions of illumination is directly pro-

portional to the quantum yield, equation (3) can be rewritten as:

$$\frac{I_o}{I} = \frac{K_a + K_q P}{K_a + K_q P_o} \quad (4)$$

Using a short hand notation we have:

$$\frac{I_o}{I} = A + B \left(\frac{P}{P_o} \right) \quad (5)$$

Where:

$$A = \frac{K_a}{K_a + K_q P_o} \quad (6)$$

$$B = \frac{K_q P_o}{K_a + K_q P_o}$$

Equation (5) is the equation that will be used in this study to generate a continuous pressure map with respect to the intensity level of the MDA paint sample. Here P is the pressure on the model for wind-on condition, P_o is the known reference pressure (wind-off condition). Note in passing that A and B adds up to one. This will serve as an index of goodness to judge the calibration curves. A and B are the paint luminescence sensitivity coefficients. The ratio of the paint emitted intensity for wind-off over wind-on compensate for such phenomena like non-uniformities of the illumination intensity and the coating thickness of the sample. It should, also, be pointed out that the paint luminescence sensitivity coefficients (A and B) are temperature dependent.

Now let's go one step further with the above equations since aerodynamicists usually use a dimensionless pressure, C_p termed the pressure coefficient, in assessing the influence of the different aerodynamic parameters. The equations above can be written in such a way that the dimensionless parameter C_p can be obtained. C_p is defined as:

$$C_p = 2 \left(\frac{P - P_o}{\rho_\infty V^2_\infty} \right) \quad (7)$$

where:

- P = static pressure at the surface of the model
- P_∞ = static pressure in the wind tunnel
- ρ_∞ = free-stream density in the wind tunnel
- V_∞ = free-stream velocity in the wind tunnel

So, let's write equation (7) in such a useful form so that either C_p or P/P_o can be calculated depending which one is known. Here, the subscripts below mean the following:

- o = ambient or stagnation condition outside the wind tunnel
- ∞ = free-stream condition of the air in the wind tunnel just ahead of the model

The following relations will be used:

- P = ρRT, equation of state (8)
- a² = γ(P/ρ), speed of sound (9)
- M = V/a, Mach number (10)

where:

$$\gamma = c_p / c_v, \text{ specific heat}$$

Now substitute equations 8 to 10 into equation 7 we obtain:

$$C_p = \left(\frac{2}{\gamma M^2_\infty} \right) \left[\frac{P_o}{P_\infty} \frac{P}{P_o} - 1 \right] \quad (11)$$

and

$$\frac{P}{P_o} = \left(\frac{P_\infty}{P_o} \right) \left[C_p \left(\frac{\gamma M^2_\infty}{2} \right) + 1 \right] \quad (12)$$

where from isentropic relation:

$$\frac{P_\infty}{P_o} = \left[1 + M^2_\infty \left(\frac{\gamma - 1}{2} \right) \right]^{\gamma / (\gamma - 1)} \quad (13)$$

Therefore, from equations 11 and 12, p/p_0 or C_p can be calculated for any M_∞ . It needs to be pointed out here that P/P_0

is the quantity that will be obtained from the calibration of the PSP sample once the image is digitized. However, if one wishes to convert P/P_0 to the C_p form for comparison with published data, equation 11 provides that flexibility.

3. PSP STRUCTURE

Pressure sensitive paint (PSP) usually consists⁶ of four polymeric layers* which are applied consecutively to the model surface. These layers are:

- Screen Layer
- First Adhesive Layer
- Second Adhesive Layer
- Active Layer

The Screen Layer: is composed of special white paint which creates an optical uniformity on the surface of the model and increases the reflection of light. This layer also creates a chemical and physical separation between the model and the active layer so that the nature of the model does not influence the properties of the PSP. The thickness of the screen layer is approximately 25 micrometers (see fig. 1).

The Adhesive Layers: are applied to assure adhesion of the active layer to the model. The thickness of each adhesive layer is about 10 micrometers.

The Active Layer: consists mainly of two compounds; one being polymer which is highly permeable to oxygen and the other being the specially developed luminescence luminophore which is dispersed within the polymer. The thickness of this layer varies between 5 to 15 micrometers.

4. PAINT CHARACTERISTIC

The paint chemistry formulation will not be discussed here since it is MDD' proprietary. In general, the compounds used for the chemical composition of the pressure sensitive paint are based on fluorescence (or phosphorescence) quenching. The characteristics that they all share are the following: they must be stable (since time is needed to make the desired measurements), they must luminesce, their luminescence must be quenched by oxygen, the luminescence, in addition, must have the appropriate life-time. The compounds which have

such characteristics⁷ are polycyclic aromatics (pyrene, decacyclene, fluoranthene, benzoperylene, ect..), porphyrins, and organic metal complexes of ruthenium, osmium, iridium, and platinum. The paint composition must contain a suitable binder (such as silicones, polyvinyl, polychloride, polymethyl, polymethacrylate, polyurethane, polystyrene, ect...) or matrix for immobilizing the compound, and it must be amenable to a suitable application method such as brushing or spraying. The samples used for this study belong to the MDA FP2B family of Mc Donnell Douglas paints and they are excited in the visible blue band. Nominal excitation band for the paint is 400-500 nm. It can be excited by both light source and laser. Possible light sources are: Xenon arc, tungsten-halogen. Laser source: argon ion laser.

The paint luminesces in a band of wavelengths centered at 600 nm. The light source must be filtered so that it emits no light in the luminescence band. Thus, a colored glass long pass filter was installed in front of the camera lens which passed wavelengths from 530 nm up. It should be stressed that the filter must remove all light except that emitted by the paint (paint luminescence). In case that lamps are used to excite the paint, additional filters need to be used in front of the lamps, but, for this investigation, only the argon ion laser was used for excitation.

The paint sample was sprayed on a thin copper plate since it could not have been sent to VKI in liquid form because it is flammable. Therefore, a lot of care was taken in glueing the thin copper plate containing the paint on the flat plate mounted with the conical fin model. The thin copper plate was glued on the plate using a 3M 467MP Hi performance double sided heat resistant adhesive.

5. EXPERIMENTAL SETUP

The PSP, illuminator, and detectors were demonstrated with a bench-top apparatus (see fig. 2) that used a small pressure vessel to test the response of the paint. The front wall of the vessel was made of glass, to allow optical access for illumination and detection. The opposite wall was coated with PSP sample and the pressure in the vessel was varied using a vacuum pump and bleed valves. The response of the paint at different pressure levels was then detected and evaluated. These levels corresponded to pressure levels expected for the VKI H3 hypersonic wind-tunnel which was used for the shock / boundary layer interaction experiment (see ref. 8).

6. EQUIPMENT USED

The paint surface was excited using a 5 watt argon ion laser (Spectra Physics- Stabilite 2017-05) which provides a maxi-

* The MDD PSP samples are made up of two layers only: the screen and the active layers.

mum of 2 watts net power output with a wavelength of 514 nanometer. The paint emission data was acquired with a 10 bit IVC-500 CCD video camera, using an f1.4/ 16 mm and a 25 mm lens, equipped with a colored glass long pass filter (Melles Griot: 03FCG087- OG550), chosen such that it passes only the paint's emission (the paint response peaks at 600 nanometer) wavelength. The camera was equipped with an internal infrared filter and the automatic gain control of the camera was disabled so that consistent light intensity was obtained throughout the test. The camera was co-located with the laser, and the output was digitized at 512x512 pixel spatial resolution and 8 bit grey level resolution using the VKI (see fig. 3a) image processing facility (DIP) equipped with a frame grabber board mounted to the VAX computer. A microscope lens with a diameter of 8.5 mm and a magnification factor of 20 was used in front of the laser in order to expand the beam so as to achieve a full coverage of the sample. A calibration chamber with optical access and equipped with a pressure gauge was used with the paint sample glued to the wall opposite of the optic glass wall. A mercury manometer was used to measure the pressure level in the calibration chamber. A pump was used to create a vacuum condition in the calibration chamber. A Sony U-matic video tape recorder and a TV monitor were used for data recording and monitoring. For some tests, an autonomous image data acquisition (see fig. 3b) and image processing system (PC-scope: the use of direct digital image storage) was used, with the purpose of eliminating the noise possibly associated with the magnetic tape recording. To assess the temperature effect on the sample response, a copper-constantan foil thermocouple was placed in the back of the flat plate containing the sample inside the chamber and a feed-through cable via a hole drilled in the center of the calibration chamber was connected to a voltmeter and a pen plotter. The temperature source incorporated a heating device connected to a copper belt containing kapton strip heaters which was wrapped around the outside of the calibration chamber for heating purposes. An ammeter was used to control the current supply.

7. DATA ACQUISITION PROCEDURE

1. Vacuum condition was established (using a pump and a mercury manometer) in the calibration chamber
2. A completely dark environment was established for the entire duration of the test (only the laser light was on)
3. Camera gain and aperture and laser power level were adjusted to avoid saturating the sample response

4. Laser net power output was measured (with a power meter)
5. A dark current (camera noise) image was recorded with the cap on the camera lens with all light source off (including the laser)
6. Laser light was turned back on but all other light sources were off
7. The sample response image for the vacuum point was recorded, then,
8. A new pressure (point) was set by using a valve between the mercury manometer line and the pressure vessel container
9. Once the desired new pressure point was set on the manometer scale, an image was recorded for that point
10. The same procedure of steps # 8-9 was followed for each new point until all the desired pressure points were obtained
11. Finally, an atmospheric pressure point was recorded for the reference pressure point (the intensity reference point)

8 DATA REDUCTION PROCEDURE

1. The experimental data recorded on a magnetic tape was imported to the DIP environment for digitization (see fig. 3a)
2. The VAX environment was coupled with a frame grabber for the digitization
3. The image for the vacuum point was displayed on the frame grabber and a set of x-y coordinates were chosen on one segment of the displayed image
4. The dark current (camera noise) image was next displayed on the frame grabber. The same x-y coordinate chosen in step 3 was set on that image as well and pixels averaging was done in the area where the x-y co-ordinate was set
5. The image for the vacuum point was redisplayed on the frame grabber and the dark current (camera noise) image was subtracted from it (the vacuum point image)
6. The new image (without the camera noise) for the vacuum point was displayed on the frame grabber and the previously chosen x-y co-ordinate was located, then, the intensity value for this image was read from the VAX terminal
7. The next image for the next pressure point was displayed on the frame grabber, the same procedure of steps 5-6 was carried out in order to read the intensity value for that image

8. The same procedure was carried out for each pressure point chosen. At the end, one ended up with intensity values and pressures correspondence

9. DISCUSSION OF CALIBRATION TESTS

9.1 Background

For this study several calibration tests were performed in order to assess some of the characteristics of the paint using an argon ion laser as the exciting source light. Two PSP samples of the same family were tested. The first one, which will be referred to as sample A, was tested to quantify the sample response under appropriate lighting as the pressure level was varied. Also, tests were conducted to assess sample degradation due to long time exposure to the excitation source, and camera noise influence on the data accuracy. All the experimental data were recorded on a U-matic magnetic tape (see fig. 3a). For the second sample (sample B), tests were conducted to assess not only the sample response but also to quantify the effect of temperature on the sample response (since the PSP luminescence coefficients A and B are temperature dependent). Also, more measurements were taken to quantify the noise contribution of the chain measurement which will undoubtedly decrease data accuracy. To carry these tests, PC Scope Image Acquisition / Processing System and the temperature equipment (which was described in section 6) were added to the original set-up (see fig. 3b). In this chapter, the results of sample A will be presented and discussed, then, the results for sample B will follow.

The values of the sensitivity coefficients (A and B) of equation (5) were obtained by measuring the pressure and temperature response of a representative luminescence paint sample over the range of conditions that was expected to be encountered in the H-3 wind tunnel test. A sample of the paint was placed in the calibration chamber and illuminated in its exciting wavelength range with an argon ion laser and its response was recorded. A wrap around heating belt was used to heat up the calibration chamber to temperatures of 15° and 35° C above ambient and a foil thermocouple was placed inside the calibration chamber in the back of the plate containing the paint sample so as to investigate the temperature influence on the paint response. The emitted intensity of the paint was measured over a range of pressures of 0 to 14 psia.

9.2 Paint Intensity Response (Sample A): Ambient Condition

Figure 4 shows the luminescence of the pressure sensitive coating (in an area of 5 pixels in the x and y direction where there was no variation in the intensity value), once exposed to oxygen and appropriate lighting. As the pressure increased,

the intensity of the light emitted by the molecules decreased as a consequence of oxygen dynamic quenching.

Since the equation that is being modelled here is equation 5 (see the theoretical part), one expects to obtain a linear response of the intensity ratio as the pressure ratio is varied. Indeed, figure 5 shows that linear dependency of intensity ratio with pressure. In that figure, intensity ratio is plotted versus pressure ratio. The intensity ratio effectively cancelled out the effects of light non-uniformity and variation in paint coating thickness, thus, improves data accuracy. P_{atm} is the known atmospheric pressure recorded before the test, P (the pressure that is being varied) also is a known pressure since it is set using the valve/manometer. I_{atm} is the reference image intensity recorded at the known atmospheric pressure and I is the image intensity recorded for P (pressure) set using the valve/manometer. From that figure, the slope and the intercept were found to be: $A = 0.9497$ and $B = 0.0576$. Theoretically, $A + B$ is expected to be 1 (equation 6). The result obtained matched rather well with the expected theoretical prediction. It can clearly see from the plot that up to a pressure ratio of 0.55, the points match the curve fit quite well. Past that threshold, data scattering is noticeable. The reason is the following. At vacuum the response of the paint (in term of luminescence) peaks out and can, therefore, easily be detected by the charged-coupled-device detectors (CCD). As the pressure increases (close to atmosphere), the paint response is barely noticeable, thus, it is much more difficult to get accurate reading from the CCD camera because the Signal to Noise Ratio (SNR) of the camera decreases which implies that the reading is polluted by the camera noise. Of course, that can be avoided by using a better grade CCD (12-14 bits), but at a higher cost.

The error approximation (figure 6) shows exactly the effect just discussed above. The error band estimation is very good near vacuum condition, but shows excessive scattering above pressure ratio of 0.50.

To improve the accuracy of the data, the reference intensity was chosen at vacuum condition (where the paint luminesces the most) instead of the atmospheric reference condition. Figure 7 clearly shows that there is an improvement in the scattering at high pressure, most of the data point match very well the curve fit.

The test was repeated three times for repeatability purpose. Figure 8 shows the result of all the three tests performed. The same trend is obtained for all the three test; scattering of the data points past a pressure ratio of about 0.50. The result shown in figure 8 is for the atmospheric reference point con-

dition, the scattering due to camera noise for all the cases is clearly noticeable.

Second, the paint was tested for degradation over time. The procedure was as follows. The laser beam continuously lit the sample over a period of forty five minutes. An image was recorded each minute while keeping the pressure constant over the forty five minutes exposure time of the paint to the continuous excitation. Figure 9 shows the result of the test. No significant degradation was observed in the paint intensity response during the forty five minutes. From a curve fit, the rate of degradation of the paint was found to be on the average of 0.3 pixel per minute. For all practical purposes that low rate of degradation can be neglected when taking into account camera noise influence, light source instability, and that only 40 frames were averaged (see fig. 12). But more importantly, in a real test case the excitation source light will be on for about 15 seconds maximum to acquire one data point, thus, degradation would most likely not be of concern. For comparison purposes, some of the pressure sensitive paints that are excited by UV light degrade⁸ by 40 to 60 % in intensity after one hour of continuous exposure to the UV light.

Third, the CCD camera noise characteristic was also assessed to quantify the noise contribution. Figure 10 shows the CCD random noise in both spatial and temporal. This is important to know since at high pressure (atmospheric), the intensity response of the paint is very low (low luminescence), thus, the camera noise influences significantly the result. Also, figure 10, points out something else. As mentioned earlier, a dark current noise image (camera with cap on) is taken at the beginning of the test and that image is subtracted from each data point to eliminate the camera noise, figure 10 shows the need for taking a dark current noise image for each point and then subtracting it from that particular data point in order to increase data accuracy.

9.3 Effect of Several Frames Averaged

For all of the figures presented above, only one frame was used in digitizing the data. Such procedure most likely introduces some inaccuracy in the result since there could be anywhere between 2 to 15 pixels intensity level from frame to frame. That difference is due partially to the light source instability, but mainly from the CCD camera random noise. Therefore, to improve the results forty frames were averaged. Figures 11 to 13 show the results. Indeed, when comparing figures 11, 12 and 13 with figures 5, 9 and 10 respectively (they are the same tests), the decrease in data scattering past a pressure ratio of 0.50 is clearly noticeable. Thus, a much better fit of the data was obtained. The averaging benefit is even more pronounced when figures 12 and 13 are compared

with figures 9 and 10 (same tests the only difference is that 40 frames are averaged in 12 and 13). The randomness in camera noise is tremendously smoothed out by the averaging process.

9.4 Paint Intensity Response (Sample B): Ambient Condition

From this point on, the result of sample B tests will be discussed. First, lets point out the difference in data acquisition between sample A and sample B. For sample B, PC-Scope and an internal VKI program were used to acquire the image. PC-scope controlled the camera, the VKI program controlled the image acquisition mode such as camera gain, offset, number of frames to acquire for one image (since only one frame can be acquired with PC-Scope). The experimental data were recorded directly to the internal PC drive in digitized form rather than acquiring the data on magnetic tape and then digitize them.

Figure 14 shows again the linear dependency of intensity ratio on pressure ratio which is a confirmation that indeed the Stern Volmer relation accurately models the paint response. Also, that figure shows that good repeatability can be obtained from sample to sample using the same batch which is something important to know since usually one sample is used for calibration and another one for the test. For this ambient calibration curve, the paint sensitivity coefficients were found to be: $A = 0.1093$ and $B = 0.8991$.

The error approximation curves (fig. 15 and 16) show the same trend discussed earlier in regard to camera random noise polluting the data accuracy at the higher end of the curve (starting at a pressure ratio of 0.6). However, with the addition of PC-Scope much less scattering is seen even in the higher end of the curve (close to atmospheric condition) compared to the previous work that was done without the use of PC-Scope. The increase in accuracy is attributed to the elimination of noise associated with the magnetic tape.

9.5 Paint Intensity Response: With Temperature Effect

Since the test was going to be performed at Mach 6, the model surface temperature was expected to rise significantly. Therefore, it was judged necessary to quantify the influence of temperature on the paint response in order to make correction for the paint sensitivity coefficients (A and B). For the test case, an overall temperature increased of 15.7 C was recorded from the thermocouple that was inserted behind the flat plate containing the paint. Figure 17 is a calibration curve showing the influence of temperature on the paint sensitivity coefficients

for 15.4 C above ambient. Compared to the ambient case, here, A was found to be 0.4049 and B to be 0.6281. Thus, the slope of the curve when temperature is taken into account, decreases from 0.8991 to 0.6281 and the intercept increases from 0.1093 to 0.40490. Since the slope decreased in the case of temperature, that would yield a lower intensity response.

The error approximation for the case of temperature influence is shown in figure 18. One thing that is clearly seen from these figures compared to the ambient condition case is the fact that at a pressure ratio of 0.1, the error approximation is much higher than for the ambient case but approximately the same by the time a pressure ratio of 1 is reached. The reason is because the Stern Volmer linear approximation response does not hold any longer when temperature effect is dominant at the low pressure (near vacuum).

Since the rise in model surface temperature for the Mach 6 case was known due to prior testing carried out using the infrared technique for the same model, tests for temperature influence were conducted from ambient up to a temperature of 30 °C above the ambient condition. Figure 19 shows the result of such test. Again, it can be seen at low pressure that the linear response predicted by the Stern Volmer relation is no longer valid. Also, the figure shows that the intensity ratio increases as temperature is increased above ambient. However, that does not mean that the raw intensity level of the paint itself increased. In fact, it is quite the opposite. Figure 20 illustrates the point quite well. In that figure the intensity response level (not the ratio) is plotted versus the pressure. As it is clearly seen, the intensity level decreases with increasing temperature. From the ambient condition, a peak intensity of 185 pixel value is obtained, by the time a temperature of 30 °C above ambient is reached, the peak intensity is dropped to only 88 pixel value.

After all these works were conducted, the preparation of the model was done and testing at the VKI H-3 wind tunnel was underway. An unexpected thing happened. The paint was no longer responding as expected to the exciting light source. In other words, it was impossible to saturate the paint even with a 2 watts net laser power output whereas before about 24 milliwatt net power output was required for near saturation. Since the paint lost almost all its sensitivity after the temperature tests, the only logical answer to the non-saturation problem was that the paint degraded in an irreversible manner. That was confirmed by placing a small unused strip of the same sample next to the sample tested for temperature effect once the laser was switched on. At about 25 milliwatt, the small strip sample was totally saturated whereas the sample tested for temperature effect was not responding at all to the exciting source light at such low laser

power setting. Therefore, another calibration tests were done to investigate to what extent the paint actually degraded since no such phenomenon has been reported in the literature so far.

9.7 Irreversible Degradation of the Paint Sample

Figures 21 and 22 show the result of the degradation test. Figure 21 presents the result in the intensity ratio vs. pressure ratio format while figure 22 characterizes it in term of pixel value vs. pressure so that the magnitude of the degradation of the paint can be seen. Both curves show the intensity response of the paint before degradation (intensity response for the ambient condition) and intensity response after the temperature tests were conducted. The peak intensity for the ambient condition has a pixel value of 185 while it has a value of 21 after the temperature tests were conducted. Thus, the paint degraded by 88.65%. What is even much more important to point out is that the degradation is totally irreversible.

9.8 Calibration Test Conclusions

The conclusions drawn from the calibration curves show above are the need to average several frames (between 40 to 100 frames) for each data point (including the camera noise) in order to improve data accuracy. Also, since camera noise is random in time and space, an averaged dark current image must be taken for each data point and then subtracted it (the averaged dark current image) from that particular point (averaged image). Finally, temperature effect must be taken into account (mainly in the case of hypersonic flows) in order to accurately capture the phenomenon being investigated as was shown above. These will be the procedure followed in carrying out the experimental test in VKI-H3 wind tunnel.

10. H-3 EXPERIMENT

10.1 Description of the H-3 Facility

The VKI hypersonic tunnel H-3 is a blow down facility with an axisymmetric nozzle giving a uniform Mach 6 free jet 12 cm in diameter. Air is supplied from a pebble-bed heater at stagnation pressures from 7 to 35 bar; the maximum stagnation temperature is 900 K. Reynolds number may be varied from 3×10^6 to $30 \times 10^6/m$. The test section contains a three-degree-of-freedom traversing mechanism for model and/or probe support, as well as a variable incidence mechanism (-5 to +5 degrees). A mechanism for rapid injection of models is available which will be used in this investigation to inject the model once the flow is established. The tunnel is equipped with mechanical scanivalves or electronic scanners for pressure measurements and a three-component strain gauge balance (see fig. 23).

10.2 Description of the Model

The occurrence of striations is observed downstream of the side fuselage reattachment line of the space shuttle Orbiter at high angle of attacks at hypersonic speed. To study the complex flow structure in that region the geometry is approximated by assuming the side fuselage of the Orbiter as a flat plate and its wing as a fin. For this study the flat plate is made of steel and its dimensions are 210 by 100 mm (length x width). A steel section forms the leading edge and extends all the way back to the trailing edge where it forms the interface to the model support. The fin is made of brass and it is mounted perpendicularly 75 mm downstream of the leading edge at an angle of attack of 40°. The fin is conical and has a maximum thickness of 5 mm, a height of 26.8 mm and a length of 100 mm. The sweep back angle investigated is 75° which is the most atrocious condition for this geometry (see fig. 24).

10.3 Experimental Setup in H-3

The same set up that was used for the calibration runs (in terms of equipment) which was described in section 6 was used for the H3 tests, except that the complete model was mounted on the injection system instead of just the flat plate in the case of the calibration runs.

11. DISCUSSION OF H-3 TEST

11.1 General Background

For the H-3 test, a scanivalve pressure system was installed in the wind tunnel in order to track accurately the reference pressure. The system is made up of two scanivales each one containing 32 pressure ports (a total of 64 pressure ports) sampling 200 data points in five seconds. A PC was used to monitor the system. The paint active area was confined to 170 mm in length (20 mm away from the plate leading edge and likewise from the trailing edge) and 100 mm in width. The model was sting mounted in the wind tunnel and the leading edge of the flat plate was positioned at 12 mm from the nozzle exit.

For the test, the flow condition was first established, then, the model was injected into the flow. Once the tunnel chamber pressure was no longer fluctuating, image acquisition was initiated via an internal VKI program which was linked to PC Scope. Twenty images were taken for each test conducted in order to be able to average the images. Image acquisition per test lasted 14 seconds for the 20 images. For the reference image (20 images), the VKI H-3 wind tunnel was pumped down to near vacuum (between 7 to 10mm Hg) since a vacuum reference image was judged to be more appropriate than an at-

mospheric one due to the limitation in resolution of the CCD camera at high pressure (that fact was pointed out early on in the calibration discussion part). The test discussed here was performed at a tunnel chamber pressure of 30 bar and a temperature of 530 K. The injection transient time for the H-3 is about 20 to 50 millisecond. That should be added to the total time of the test since heating does play a role during that transitional state. The H-3 wind tunnel uncertainties associated with such condition are: 30 bar +/- 1% stagnation pressure and stagnation temperature of 540 +/- 0.1 K. The Mach number is 6 +/- 0.1. A copper constantan foil thermocouple which was connected to a pen plotter was inserted within the plate on which the conical fin and the pressure sensitive paint were positioned in order to assess the temperature change during the test.

For the data reduction four transversal lines were chosen for analysis since there exists substantial pressure tap measurement data for the model used. The transversal lines were chosen at an axial (longitudinal) position of 90, 115, 140, 200 mm respectively from the leading edge of the flat plate. Three of the transversal lines chosen started from the conical fin at the specified x-location, and then moved away from the body to the free-stream zone. The 200 mm one was made 30 mm away from the trailing edge of the conical fin (10 mm away from the trailing edge of the flat plate). All the transversal lines were chosen on the expansion side of the model since most of the change in terms of pressure was expected to be taken place in that zone.

11.2 Comparison Between Pressure Sensitive Paint and Tap Measurement

Since pressure tap measurement data are available for the model used, they will be used as a basis for comparing the results obtained using the pressure sensitive paint. The results shown using pressure sensitive paint are plotted in the flat plate physical dimensions. However, only the active area (where the pressure sensitive paint was laid) is taken into consideration even though all the transversal lines position are referenced from the leading edge of the flat plate.

Figure 25 shows the comparison between the pressure tap and pressure sensitive paint measurements. The square symbol represents the pressure sensitive paint and the diamond shape symbol represents the pressure tap measurement. The y-coordinate represents the physical location on the flat plate for a specific x location. In this case, the x-position chosen was located 200 mm from the leading edge of the flat plate (or 10 mm away from the trailing edge). For a y-value of 80, this is on or close to the conical fin model. And for a y-value of 20, this is in or close to the free stream. The x-coordinate repre-

sents the pressure which is normalized by the free stream pressure (1931 n/m^2). As it is clearly seen, there is a significant difference between what is measured by the pressure tap and the pressure sensitive paint. However, it can be seen that both data set show the same trend; the peaks and valleys match very closely except that there is a shift when it comes to the actual value itself. The reason of this shift is still elusive up to this moment. Therefore, all the possibilities (causes) are being looked into to determine the reasons why. The causes being looked into are whether there is a systematic error, a much greater temperature influence than recorded due to the use of the adhesive to glue the PSP sample to the flat plate, the camera resolution not good enough to detect the actual change in intensity for a change in pressure or could it be an aging effect on the paint since the samples were used after a year after being sprayed on the copper sheets. For this test a localized bulk temperature change of $15^\circ.7$ was recorded from the thermocouple reading. Due to the adhesive layer this may not accurately reflect the temperature of the paint.

Figures 26 and 27 show exactly the same trend with figure 25. They were done for a x-position of 140 and 115 mm away from the leading edge respectively. The peaks and valleys seem to coincide but the data is shifted by approximately the same factor as in figure 25. This leads to the conclusion that a systematic error is present or paint aging might be a factor that needs to be considered.

11.3 Camera Resolution Assessment

Figure 14 is the calibration curve redone taking into account only the pressure range in which the H-3 test was performed. Figures 15 and 16 represent the approximate error or the error band associated with figure 14. From these three figures one clearly sees that the scattering in the lower part is much lower than in the upper part of the curve which is the trend that was expected. Also, looking closely at the data one can see that the camera can, indeed, pick up the correct signal since the variation for a certain change in pressure correspond to a certain variation in intensity. The variation in intensity over the pressure range the test was performed is about 15%. The CCD camera used for the test is able to pick up such a change in intensity. Therefore, this put to rest the possibility that camera resolution could explain why there exists a shift in the data obtained using the pressure sensitive paint technique.

All the other possible causes mentioned earlier that might have caused the shift between the expected values for the pressure ratio and the obtained values are currently under more investigation in order to pinpoint exactly which one is responsible for the shift since the uncertainties associated with the experimental data and the facility used are too low to

make up for the difference percentage wise between the tap measurement and the PSP measurement.

12. FUTURE WORK

This study has barely scratched the surface of what needs to be accomplished in this new field. It has raised more questions than giving answers. For example, answers need to be found to the question raised in this study as to what is the temperature threshold at which the paint degradation becomes irreversible? Also, how long can the paint be exposed to such temperature before its degradation becomes irreversible? Other questions like: is that irreversible degradation paint (chemistry) dependent? Does the thickness of the paint itself play any role in all these? Last, but not least, what is the role of paint aging, if any? As one can see more work needs to be done in order to answer these questions and the ones that will come up in the process of finding answers to the questions formulated above.

13. CONCLUSION

For this study, the calibration curve obtained using the samples from McDonnell Douglas agreed with the linear response predicted by the Stern Volmer relation when no temperature effect is present. However, in the case of temperature effect (which is the case for hypersonic flows), the study showed that the Stern Volmer relation is no longer valid in the lower part of the curve (but still good past a certain point). Therefore, a second order or better yet a third order of the Stern Volmer relation must be used in order to accurately determine the paint sensitivity coefficients (A and B). In addition, it was shown that the paint degraded in an irreversible manner past a temperature threshold when exposed over a period of time (this has not been reported so far in the literature). Camera noise was shown to be important and the benefit of averaging images was clearly shown. Finally, tests at hypersonic speed (Mach 6) were performed to investigate the shock / boundary layer interaction for a flat plate / cone fin configuration model and the results were compared with the tap measurement technique.

The test result is for the moment inconclusive since there is an unexplainable shift in the result obtained using the pressure sensitive paint compared to the result obtained using the tap measurement technique. However, the trend for both pressure sensitive paint and tap pressure measurement agreed very well. Further work is under investigation to find the cause (s) of the shift in the data.

ACKNOWLEDGMENTS

This study was carried out at the von Karman Institute for Fluid Dynamics through a von Karman fellowship and the support of the US Air Force. The authors would like to thank Mc Donnell Douglas and Mr. Roger C. Crites for providing the samples used for this study.

REFERENCES

1. M. Erisman and K. W. Neves, Sc. AM. 257, 163 (1987)
2. A. Jameson, Science 245, 361 (1989)
3. J. I. Peterson and R.V. Fitzgerald, Rev. Sci. Instrum. 51, 670 (1980)
4. Janet Kawandi et al., Rev. Sci. Instrum. 61, 3340 (1990)
5. H. H. Willard, L. L. Merrit, J. A. Dean, and F. A. Settle, Instrumental Methods of Analysis (Wadsworth, Belmont, 1981), pp. 6-9
6. R. C. Crites, Von Karman Institute for Fluid Dynamics short course series on Measurement Techniques, April 19-23, 1993
7. Arne Vollan and Omegmbh, IEEE. 30, 10 (1991)
8. Kenol Jules and al., Utilisation of Pressure Sensitive Paint for the Study of Shock/Boundary Layer Interaction at Mach 6, von Karman Institute for Fluid Dynamics, Project Report 1994-35, June, 1994
9. M. J. Morris and al., AIAA Journal. 31, 419 (1993)
10. Crites, R. C. et al., Wind Tunnels & Wind Tunnel Test Techniques. 1992, ISBN 1 85768050 2
11. Bradley S. Sealey et al., An Automated Pressure Data Acquisition System For Evaluation Of Pressure Sensitive Paint Chemistries, ISA, 1993

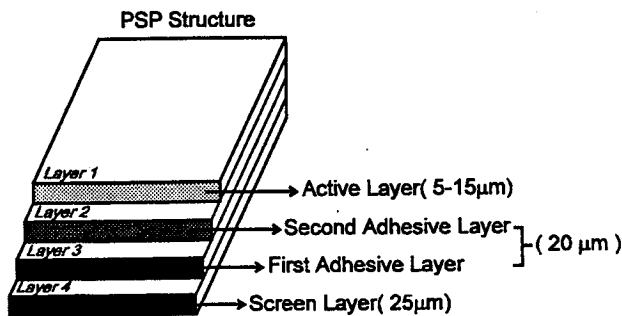


Fig. 1: Generic Pressure Sensitive Paint Structure

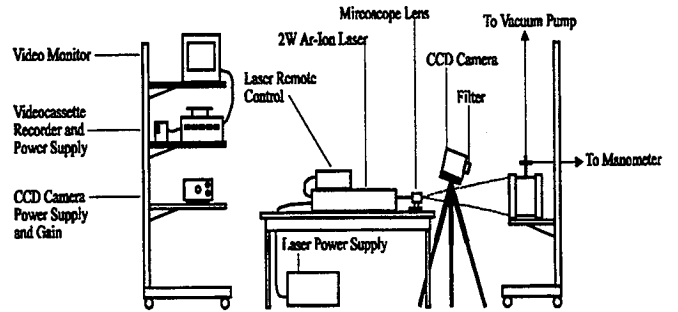


Fig. 2: Pressure Sensitive Paint Calibration Setup

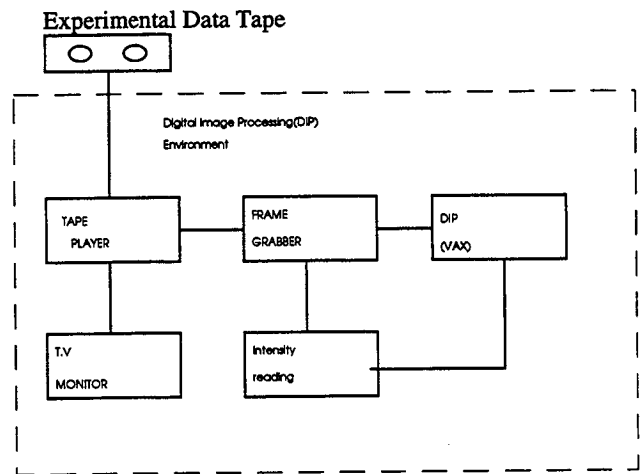


Fig. 3a: Image Digitization Environment

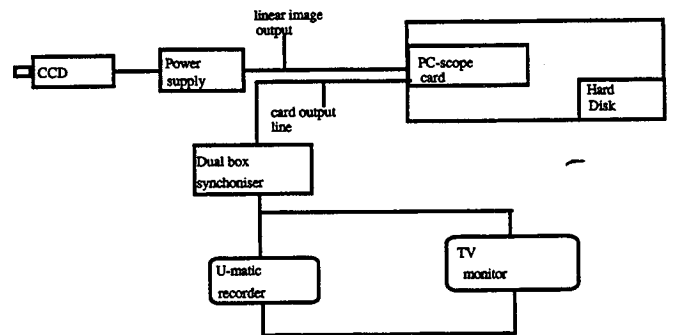


Fig. 3b: Image Acquisition Environment

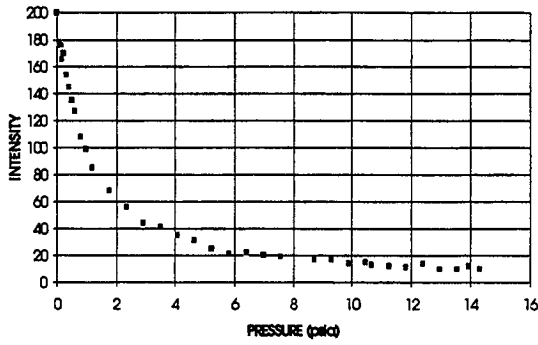


Fig. 4: PSP Raw Intensity Response with Pressure Variation

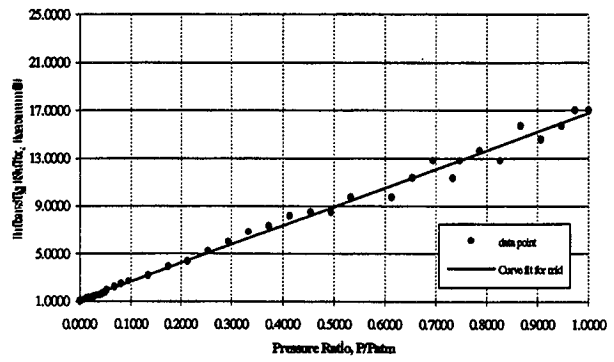


Fig. 7: Intensity Ratio vs. Pressure Ratio Using Vacuum Reference Point

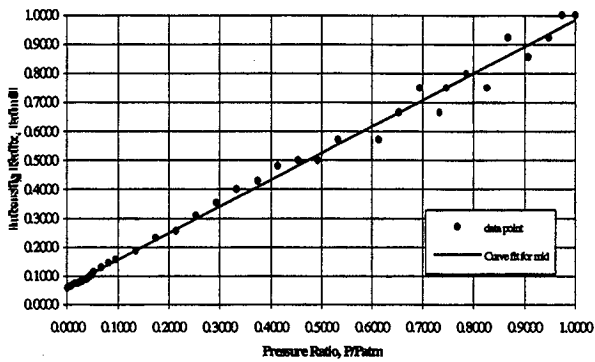


Fig. 5: Intensity Ratio vs. Pressure Ratio

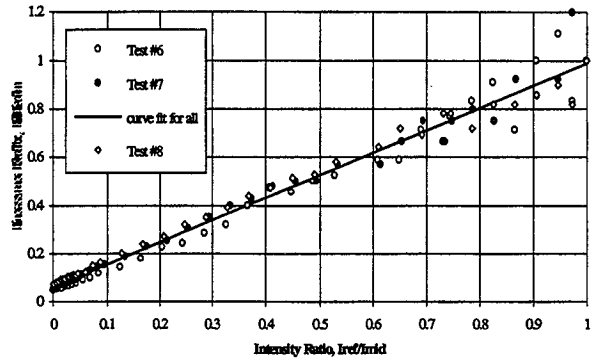


Fig. 8: Pressure Ratio vs. Intensity Ratio for Three Calibration Runs (Repeatability)

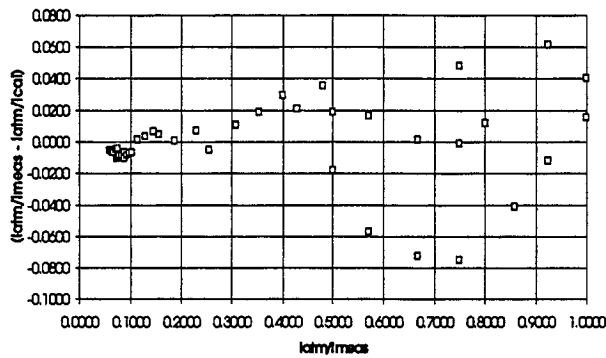


Fig. 6: PSP Calibration Error Approximation

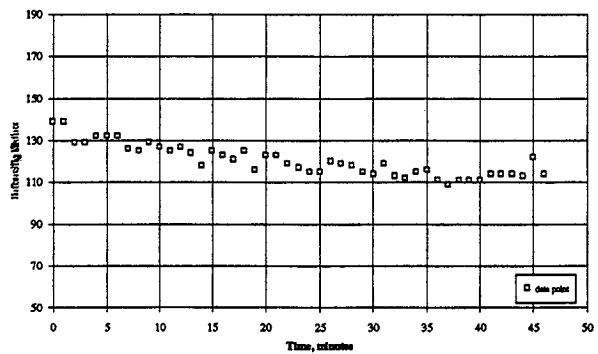


Fig. 9: Intensity Value vs. Time (PSP degradation characteristic)

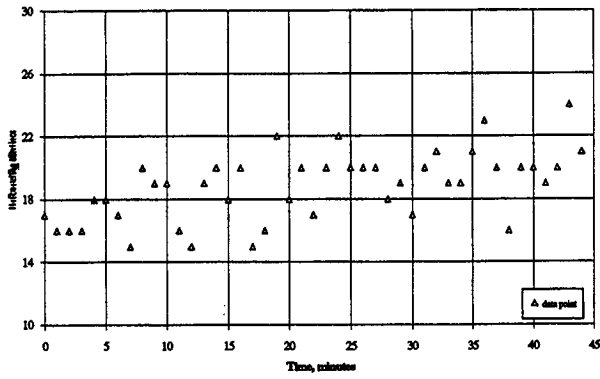


Fig. 10: Intensity Value vs. Time (CCD noise characteristic)

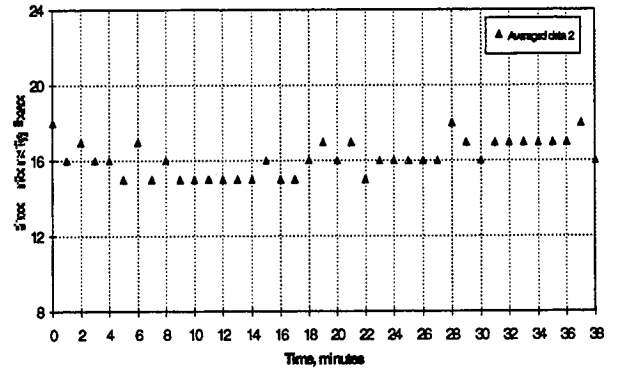


Fig. 13: Intensity Value vs. Time for the CCD Noise Characteristic (40 frames averaged)

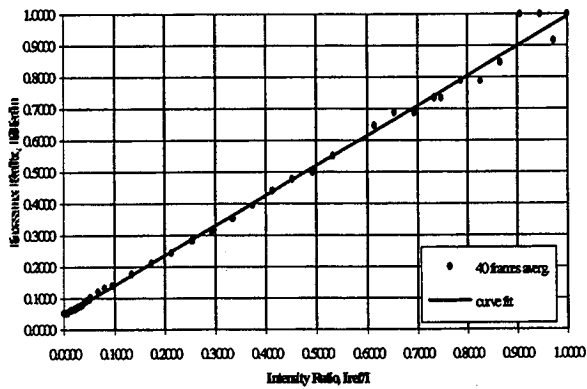


Fig. 11: Pressure Ratio vs. Intensity Ratio (40 frames averaged)

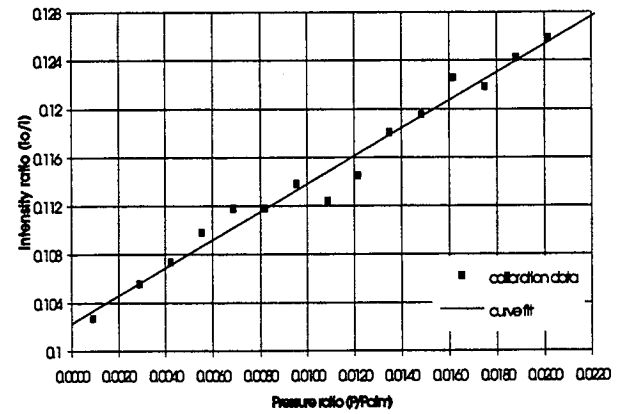


Fig. 14: Intensity Ratio vs. Pressure Ratio (calibration curve)

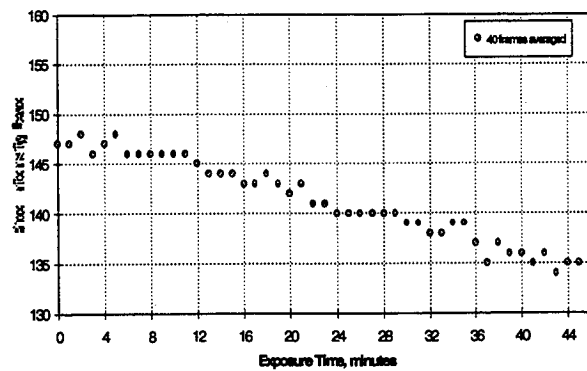


Fig. 12: Intensity Value vs. Time for the Paint Degradation Characteristic (40 frames averaged)

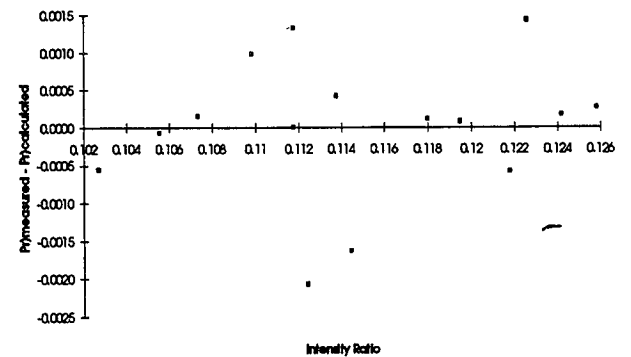


Fig. 15: Error Approximation Pressure Ratio)measured - calculated vs. Intensity

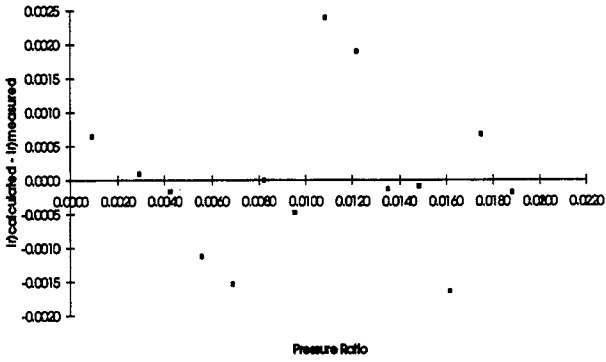


Fig. 16: Error Approximation Intensity Ratio)measured-calculated vs. Pressure Ratio

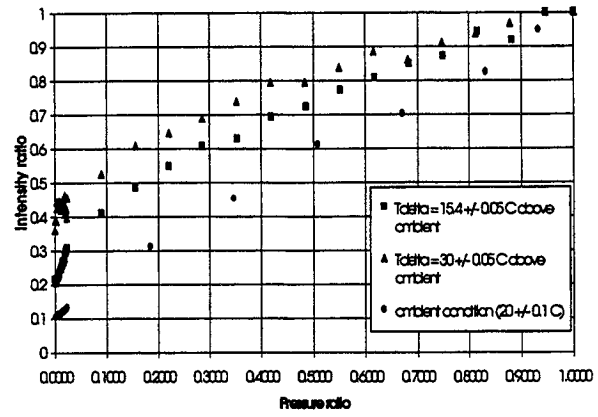


Fig. 19: Temperature Effect on Paint Intensity Response (intensity ratio vs. pressure ratio)

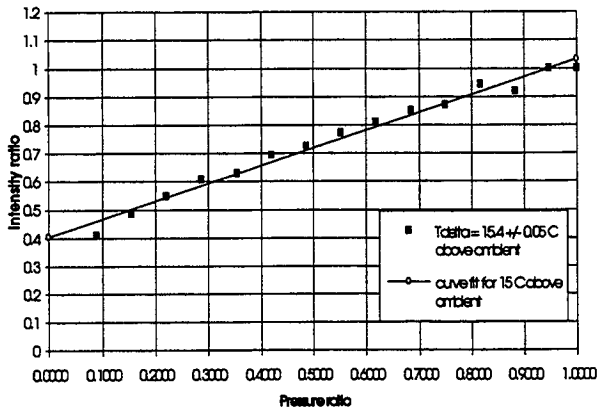


Fig. 17: Temperature Effect on Paint Sample Intensity Response

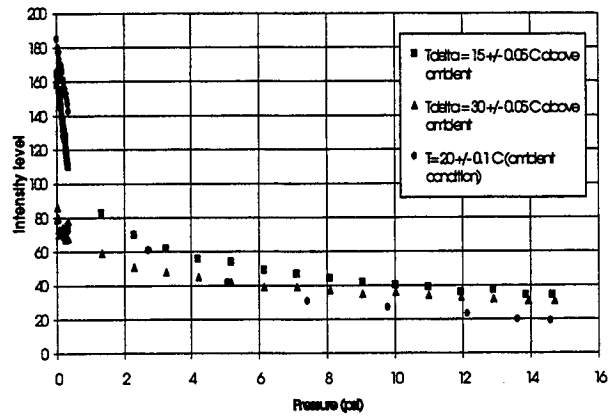


Fig. 20: Temperature Effect on Paint Intensity Response (raw intensity level vs. pressure)

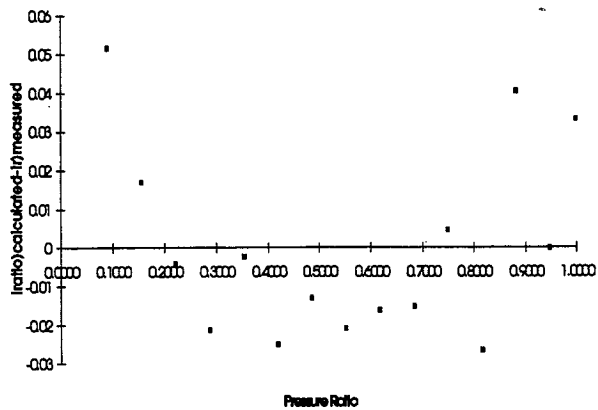


Fig. 18: Error Approximation (with temperature effect: T=15.4 °C above ambient condition)

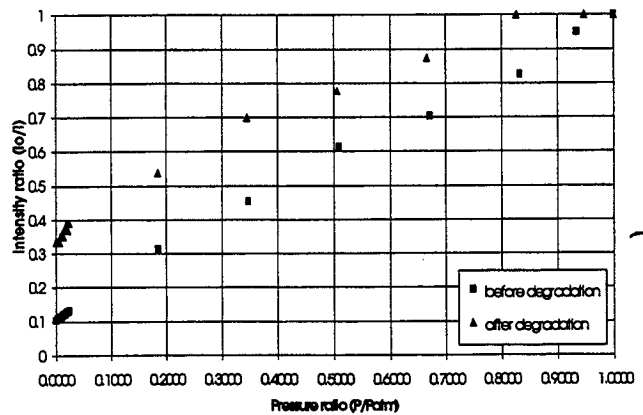


Fig. 21: Paint Degradation Due to Temperature Effect (intensity ratio vs. pressure ratio)

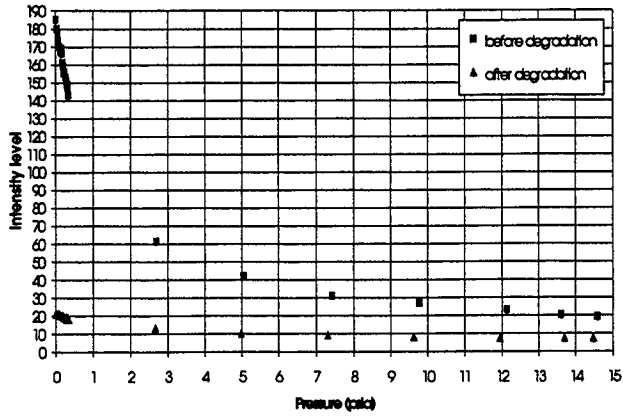


Fig. 22: Paint Degradation Due to Temperature Effect (raw intensity vs. pressure)

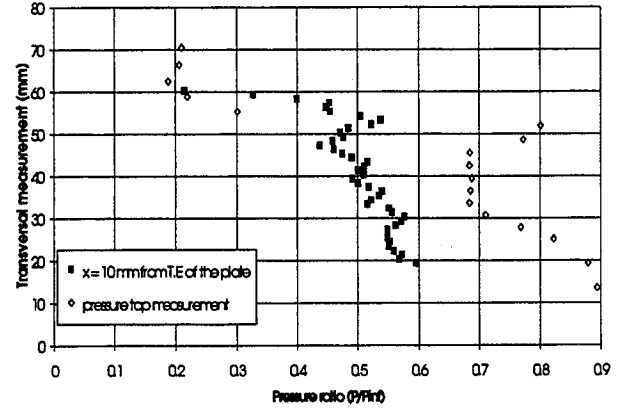


Fig. 25: Pressure Sensitive Paint and Pressure Tap Measurement at a Position X = 200 mm

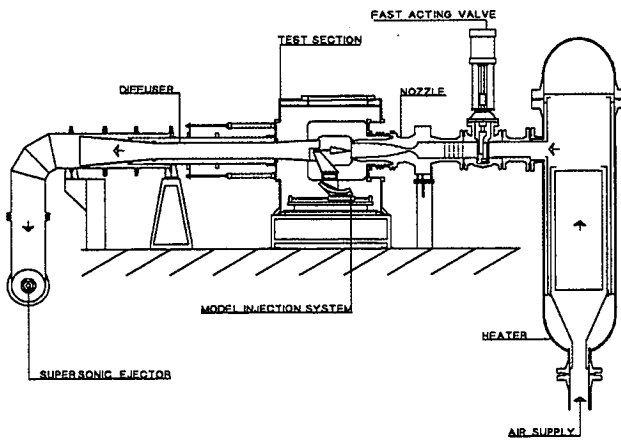


Fig. 23: Schematic Diagram of VKI H-3 Wind Tunnel

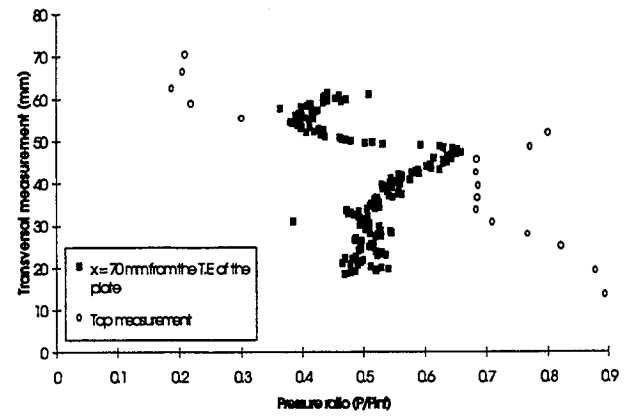


Fig. 26: Pressure Sensitive Paint and Pressure Tap Measurement at a Position X = 140 mm

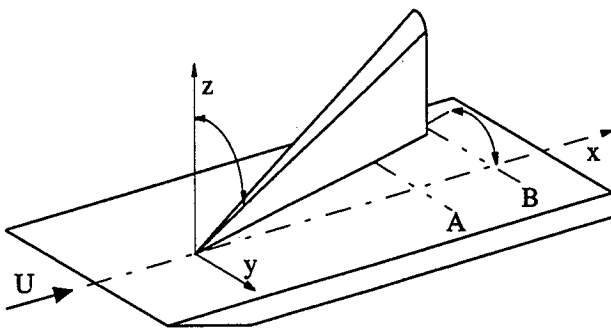


Fig. 24: Schematic of the Flat Plate/ Fin Configuration Model

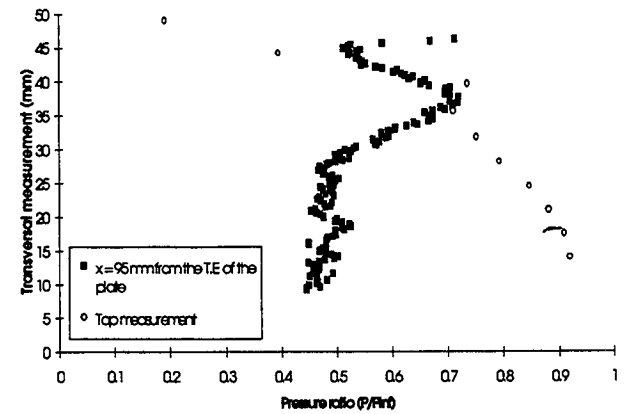


Fig. 27: Pressure Sensitive Paint and Pressure Tap Measurement at a Position X = 115 mm

REPORT DOCUMENTATION PAGE

Form Approved
OMB No. 0704-0188

Public reporting burden for this collection of information is estimated to average 1 hour per response, including the time for reviewing instructions, searching existing data sources, gathering and maintaining the data needed, and completing and reviewing the collection of information. Send comments regarding this burden estimate or any other aspect of this collection of information, including suggestions for reducing this burden, to Washington Headquarters Services, Directorate for Information Operations and Reports, 1215 Jefferson Davis Highway, Suite 1204, Arlington, VA 22202-4302, and to the Office of Management and Budget, Paperwork Reduction Project (0704-0188), Washington, DC 20503.

1. AGENCY USE ONLY (<i>Leave blank</i>)	2. REPORT DATE February 1995	3. REPORT TYPE AND DATES COVERED Technical Memorandum	
4. TITLE AND SUBTITLE Application of Pressure Sensitive Paint in Hypersonic Flows		5. FUNDING NUMBERS WU-466-05-02	
6. AUTHOR(S) Kenol Jules, Mario Carbonaro and Stephan Zemsch			
7. PERFORMING ORGANIZATION NAME(S) AND ADDRESS(ES) National Aeronautics and Space Administration Lewis Research Center Cleveland, Ohio 44135-3191		8. PERFORMING ORGANIZATION REPORT NUMBER E-9373	
9. SPONSORING/MONITORING AGENCY NAME(S) AND ADDRESS(ES) National Aeronautics and Space Administration Washington, D.C. 20546-0001		10. SPONSORING/MONITORING AGENCY REPORT NUMBER NASA TM-106824	
11. SUPPLEMENTARY NOTES Kenol Jules, NASA Lewis Research Center; Mario Carbonaro and Stephan Zemsch, von Karman Institute for Fluid Dynamics, 72 Chaussee de Waterloo, B-1640 Rhode-St-Genese, Belgium. Responsible person, Kenol Jules, organization code 2420, (216) 433-7016.			
12a. DISTRIBUTION/AVAILABILITY STATEMENT Unclassified - Unlimited Subject Category 02 This publication is available from the NASA Center for Aerospace Information, (301) 621-0390.		12b. DISTRIBUTION CODE	
13. ABSTRACT (<i>Maximum 200 words</i>) It is well known in the aerodynamic field that pressure distribution measurement over the surface of an aircraft model is a problem in experimental aerodynamics. For one thing, a continuous pressure map can not be obtained with the current experimental methods since they are discrete. Therefore, interpolation or CFD methods must be used for a more complete picture of the phenomenon under study. For this study, a new technique was investigated which would provide a continuous pressure distribution over the surface under consideration. The new method is pressure sensitive paint. When pressure sensitive paint is applied to an aerodynamic surface and placed in an operating wind-tunnel under appropriate lighting, the molecules luminesce as a function of the local pressure of oxygen over the surface of interest during aerodynamic flow. The resulting image will be brightest in the areas of low pressure (low oxygen concentration), and less intense in the areas of high pressure (where oxygen is most abundant on the surface). The objective of this investigation was to use pressure sensitive paint samples from McDonnell Douglas (MDD) for calibration purpose in order to assess the response of the paint under appropriate lighting and to use the samples over a flat plate/conical fin mounted at 75° from the center of the plate in order to study the shock/boundary layer interaction at Mach 6 in the Von Karman wind-tunnel. From the result obtained it was concluded that temperature significantly affects the response of the paint and should be given the uppermost attention in the case of hypersonic flows. Also, it was found that past a certain temperature threshold, the paint intensity degradation became irreversible. The comparison between the pressure tap measurement and the pressure sensitive paint showed the right trend. However, there exists a shift when it comes to the actual value. Therefore, further investigation is under way to find the cause of the shift.			
14. SUBJECT TERMS Luminescence; Phosphorescence; Photons; Fluorescence; Acquisition; Coupled-device-detectors; Striation			15. NUMBER OF PAGES 17
			16. PRICE CODE A03
17. SECURITY CLASSIFICATION OF REPORT Unclassified	18. SECURITY CLASSIFICATION OF THIS PAGE Unclassified	19. SECURITY CLASSIFICATION OF ABSTRACT Unclassified	20. LIMITATION OF ABSTRACT